Published in final edited form as:
Traffic. 2014 February ; 15(2): 212–229. doi:10.1111/tra.12135.

Binding to any ESCRT can mediate ubiquitin-independent cargo sorting

Shrawan Kumar Mageswaran[1], **Megan Gorringe Dixon**[2], **Matt Curtiss**[1], **James P. Keener**[2], and **Markus Babst**[1,*]

[1]Center for Cell and Genome Science and Department of Biology, University of Utah, 257 South 1400 East, Salt Lake City, Utah 84112, USA

[2]Department of Mathematics, University of Utah, 155 South 1400 East, Salt Lake City, Utah 84112, USA

Abstract

The ESCRT machinery is known to sort ubiquitinated transmembrane proteins into vesicles that bud into the lumen of multivesicular bodies (MVBs). Although the ESCRTs themselves are ubiquitinated they are excluded from the intraluminal vesicles and recycle back to the cytoplasm for further rounds of sorting. To obtain insights into the rules that distinguish ESCRT machinery from cargo we analyzed the trafficking of artificial ESCRT-like protein fusions. These studies showed that lowering ESCRT-binding affinity converts a protein from behaving like ESCRT machinery into cargo of the MVB pathway, highlighting the close relationship between machinery and the cargoes they sort. Furthermore, our findings give insights into the targeting of soluble proteins into the MVB pathway and show that binding to any of the ESCRTs can mediate ubiquitin-independent MVB sorting.

Introduction

The multivesicular body (MVB) pathway is part of the endosomal system of eukaryotic cells. It is responsible for the delivery of transmembrane proteins into the lumen of lysosomes/vacuoles where these proteins are degraded (reviewed in (1)). As such, the MVB pathway represents the major degradation pathway for transmembrane proteins in eukaryotes. In addition, the MVB pathway traffics lysosomal/vacuolar hydrolases and thus plays an important role in maintaining the function of lysosomal compartments. With a few exceptions, the sorting of cargo into the MVB pathway has been shown to be dependent on ubiquitination (reviewed in (2)). On the endosome, ubiquitinated-transmembrane cargoes are recognized by a group of protein complexes called ESCRTs (Endosomal Sorting Complex Required for Transport), which sort these cargo proteins into the intraluminal vesicles (ILVs) of the MVB (reviewed in (3)).

The ESCRT machinery consists of five protein complexes: ESCRT-0, ESCRT-I, ESCRT-II, ESCRT-III and the Vps4 complex. These protein complexes are recruited from the cytoplasm and assemble on the MVB into a protein network that is involved both in ILV formation as well as sorting of cargo into the ILVs. Deletion analyses suggested a linear order in both assembly and function of the ESCRT machinery: ESCRT-0 is acting upstream of ESCRT-I, which then activates ESCRT-II, which subsequently recruits ESCRT-III and the Vps4 complex (Figure 1A, reviewed in (4)). Several ubiquitin-binding sites have been

*Corresponding author: Markus Babst babst@biology.utah.edu.

Conflict of Interest: The authors declare that they have no conflict of interest.

identified in ESCRT-0, ESCRT-I and ESCRT-II indicating that these 'early' ESCRTs are the main cargo-binding complexes of the MVB sorting machinery (2). ESCRT-III subunits oligomerize on membranes into spiral-shaped polymers that are able to deform the underlying membrane into tubular structures (5–9). Therefore, ESCRT-III has been suggested to function in the invagination of the membrane and the abscission reaction that severs the neck between the forming ILV and the limiting membrane (10).

Even though the ESCRT machinery is directly involved in both the formation of ILVs as well as the sorting of membrane proteins into these vesicles, the ESCRT proteins remain cytoplasmic and are not packed into the lumen of ILVs. This observation is surprising considering that the ESCRTs localize to endosomes in part by binding to phosphatidylinositol-3-phosphate (PI-3P), a lipid that enters ILVs (11–15). Furthermore, studies have shown that ESCRTs are ubiquitinated (16, 17), a modification that is thought to cause efficient sorting into ILVs. These findings pose the question: What differentiates cargo from machinery? In fact, several studies have indicated that the ESCRTs are, at least to some extent, treated similarly to cargo proteins. These studies showed the regulated degradation of ESCRT-I via the MVB pathway (18). Furthermore, analysis of exosomes, extracellular vesicles that originate from MVBs, identified ESCRT proteins as constituents of these vesicular carriers (19). Finally, the deletion of the gene encoding for the ESCRT-I subunit Mvb12 resulted in the delivery of mutant ESCRT-I to the lumen of the vacuole, suggesting that this mutation caused ESCRT-I to behave more like cargo than machinery (20). Together, these observations confirm the close relationship between the ESCRTs and the cargo they sort. The three-dimensional structure of most of the ESCRT machinery has been elucidated. The interactions between the ESCRTs are also well studied. However, the spatial and temporal organization of the ESCRT network that allows for sorting of cargo into ILVs without entrapment of the machinery remains enigmatic. Therefore, the goal of this study was to obtain insights into the rules that govern ESCRT interactions and cargo sorting. We analyzed the behavior of artificial protein fusions designed to mimic ESCRTs. The results from these experiments revealed a surprisingly flexible and simple ESCRT system that differentiates between cargo and machinery simply by interaction strength.

Results

Like cargo, ESCRTs are ubiquitinated and localize to the endosomal membrane but remain at the limiting membrane of the MVB, and upon completion of MVB formation, recycle back to the cytoplasm for additional rounds of sorting. To identify the parameters for this behavior, we constructed a series of fusion proteins that mimic both ESCRT localization to the endosome and interaction with other ESCRT machinery. These fusion proteins contained well-defined membrane and ESCRT interaction domains, thereby minimizing the possibility of unknown interactions that might skew the results. Because of the complexity of interactions within the ESCRT machinery, we considered the use of ESCRT-like proteins to be more informative than mutagenesis of ESCRT components.

For endosome association, the ESCRT-like constructs contained the C-terminal region of EEA1, a region that consists of a FYVE domain and a dimerization domain (Figure 1B). The FYVE domain, which is also present in the ESCRT-0 subunit Vps27, binds specifically to the head group of phosphatidyl-3-phosphate (PI3P), a lipid enriched in endosomal membranes (13, 14, 21, 22). Furthermore, the dimerization of the FYVE domain increases the affinity of the fusion protein to endosomes (23). As expected from previous studies (14), GFP-FYVE expressed in yeast colocalized with the ESCRT-III-associated factor Ist1-RFP to small structures adjacent to the vacuole, which represent MVBs or late endosomes (Figure 2A). But unlike Ist1-RFP, GFP-FYVE also localized to the vacuolar membrane suggesting that GFP-FYVE was not recycled like ESCRTs but remained associated with the

membrane for a prolonged time, even after fusion of MVBs to the vacuole (Figure 2A). However, we are not able to exclude the possibility that some of the GFP-FYVE is directly recruited to the vacuolar membrane. The vacuolar lumen was mostly devoid of GFP, indicating that GFP-FYVE was not a cargo of the MVB pathway and thus did not contain an MVB sorting signal. Together, the microscopy data suggested that GFP-FYVE associated with endosomes but did not interact with the ESCRT machinery, properties that are essential for our studies of the ESCRT-mimics.

We fused a set of different ESCRT-interacting domains (EIDs) to the N-terminus of GFP-FYVE. These domains belong to ESCRT proteins and are known to interact with other proteins of the ESCRT machinery (Figures 1A and 1B, Table 1). The resulting ESCRT mimics were expressed in yeast and CPY-Invertase sorting assays indicated that none of the fusion proteins exhibited a dominant-negative effect on the MVB pathway, suggesting that the fusion proteins did not interfere with normal ESCRT function (Table 2). However, when overexpressed from a high-copy plasmid the EID-GFP-FYVE proteins caused MVB sorting defects (data not shown). Quantitative analysis of fluorescence microscopy pictures was used to determine the effects of the ESCRT-interacting domains on GFP-FYVE localization. The localization of each fusion protein was compared to those of the well-studied proteins GFP-Dap2, GFP-Cps1 and Ist1-GFP. Dap2 is a vacuolar peptidase (also called DPAP B) that upon synthesis traffics via the MVB to the vacuolar membrane without interacting with the ESCRT machinery (referred to as ‘non-interacting’;(24, 25). In contrast, GFP-Cps1, a vacuolar protein that is efficiently sorted via the MVB pathway into the lumen of the vacuole (25), served as an example of a cargo protein. Finally, the ESCRT protein Ist1-GFP represented the ESCRT machinery. This fusion protein localizes to MVBs by binding to ESCRT-III and upon completion of MVB formation recycles back to cytoplasm (26). As a consequence, Ist1-GFP is found on late endosomes and in the cytoplasm of the cell. Together, these three proteins represented the three possible outcomes for an MVB-associated protein, namely ‘non-interacting’, ‘cargo’ and ‘machinery’.

For each EID-GFP-FYVE, pictures of approximately 50 cells were taken and the GFP intensity of late endosomes, vacuolar membrane and vacuolar lumen was determined. In the cases where the vacuolar membrane signal was too low to be separable from vacuolar lumen (membrane staining is less or equal to that of the lumen), the value of the vacuolar membrane was set to be equal to that of the lumen. The resulting data were used to calculate for each cell the ratios of ‘vacuolar lumen-to-vacuolar membrane’ and ‘vacuole-to-total signal’ (Figure 2B). An example of these calculations is shown in Figure 2C. Notice that because the vacuolar membrane signal is never lower than that of the lumen, the ‘vacuolar lumen-to-vacuolar membrane’ ratio cannot be above 1. The ratios were then compared to those of GFP-Dap2, GFP-Cps1 and Ist1-GFP. To simplify the presentation of the data, the ‘vacuolar lumen-to-vacuolar membrane’ and ‘vacuole-to-total signal’ ratios of the standard proteins (GFP-Ist1, GFP-Cps1, GFP-Dap2) were plotted on a scatter-plot and areas were defined that contained at least 90% of the cells expressing a particular standard fusion protein (Figures 2B and 2D). These defined areas were then used to determine to which group (non-interacting, cargo, machinery) a particular ESCRT-mimic expressing cell belonged (summarized in Figure 1A and Table 1).

Binding to ESCRT-III can mediate recycling or MVB sorting

The first ESCRT mimic we tested was MIT-GFP-FYVE, a fusion protein containing the ESCRT-III-binding domain of Vps4 (27). MIT-GFP-FYVE localized almost exclusively to late endosomal compartments, which is in contrast to GFP-FYVE that localized to both endosomes and vacuolar membranes (Figure 3A). This difference in localization suggested that MIT-GFP-FYVE was removed from the MVBs before fusion to the vacuole occurred, a behavior that mimicked the recycling observed with ESCRT components. Therefore, MIT-

GFP-FYVE behaved similar to proteins of the ESCRT machinery, a result that is reflected in the quantitative analysis which indicated that >90% of cells belong to the 'machinery' group (Figure 3A). This observation also indicated that the MIT - ESCRT-III interaction was strong enough to compete with the FYVE - PI-3P interaction, causing MIT-GFP-FYVE together with ESCRT-III subunits to be pulled of the endosomal membrane in a Vps4-dependent manner.

The MIT domain was mutated to test if recycling of MIT-GFP-FYVE is indeed dependent on the interaction with ESCRT-III. The MIT domain is able to bind simultaneously to two distinct motifs in ESCRT-III, called MIM1 (MIT Interaction Motif 1) and MIM2 (27). Mutating isoleucine at position 18 of the MIT domain to an aspartate (MIT(I18D)) has been shown to impair the MIM2 interaction with ESCRT-III (28). The I18D mutation caused a slight decrease in the recycling of MIT-GFP-FYVE from the endosome, consistent with the idea that the interaction with ESCRT-III is important for the machinery-behavior of MIT-GFP-FYVE (Figure 3A). The rather weak phenotype of the I18D mutation is consistent with previous studies that showed a mild defect in MVB sorting in cells expressing *vps4(I18D)* (28). Surprisingly, mutating the MIM1 interaction site of the MIT domain (MIT(L64D)) resulted in a fusion protein that was not recycled from the endosome but efficiently sorted into the MVB pathway, mimicking cargo (Figure 3A). Expressing MIT(L64D)-GFP-FYVE in *rsp5-1*, a strain mutated for the E3 enzyme responsible for ubiquitination of MVB cargoes (29), caused only a slight defect in the sorting of the fusion protein into the lumen of the vacuole (Figure 3B), suggesting that MVB sorting of MIT(L64D)-GFP-FYVE was not due to ubiquitination of the fusion protein. This notion was further supported by the finding that expressing Hse1-DUB did not block the sorting of MIT(L64D)-GFP-FYVE into the MVB pathway (Figure 3B). Hse1-DUB is a fusion protein that has been shown to efficiently deubiquitinate endosomal cargoes thereby inhibiting their entry into the MVB pathway (30). Because a complete lack of ubiquitinated cargo interferes with ESCRT function (30), a Mup1-ubiquitin fusion was co-expressed with Hse1-DUB in cells used for MVB trafficking experiments. Together, the data indicated that sorting of MIT(L64D)-GFP-FYVE into ILVs is largely independent of ubiquitination but mediated by binding to ESCRT-III. In contrast, proper sorting of a GFP-Dap2 fusion protein containing a ubiquitination site (US-GFP-Dap2) was found to be strongly defective in the *rsp5-1* mutant strain or in presence of Hse1-DUB (data not shown), a result that is consistent with a defect in ubiquitin-dependent sorting in these strains (Figure 4D). Sorting of MIT(L64D)-GFP-FYVE into ILVs was dependent on a functional ESCRT machinery since deletion of the essential ESCRT factor *VPS4* blocked delivery into the vacuolar lumen (Figure 3B).

The idea that MIT(L64D)-GFP-FYVE is sorted into ILVs by binding to ESCRT-III was further tested by mutating both ESCRT-III interaction sites of the MIT domain. The resulting fusion protein MIT(I18D,L64D)-GFP-FYVE showed in most cells a localization pattern of a 'non-interacting' protein, consistent with the idea that this fusion protein lost most of its interactions with ESCRT-III and thus was no longer sorted into the MVB pathway (Figure 3A). However, in approximately 35% of the cells, MIT(I18D,L64D)-GFP-FYVE did sort into the vacuolar lumen, albeit inefficiently, suggesting that this fusion protein maintained some interaction with the ESCRT machinery, either with ESCRT-III or with another unknown binding partner.

The difference in behavior of wild-type and mutant MIT-GFP-FYVE constructs (machinery versus cargo) could not be explained by the different type of ESCRT-III interaction, because mutating either the MIM1 or MIM2 binding site caused reduced recycling of the fusion protein. In contrast, changes in the strength of ESCRT-III interaction were able to explain the different behaviors of the MIT-GFP-FYVE fusions. Previous studies suggested that the ESCRT-III affinity of the different MIT domains follows the order: MIT > MIT(I18D) >

MIT(L64D) > MIT(I18D,L64D) (28). Our data indicated that lower ESCRT-III affinities result in decreasing efficiency of MIT-GFP-FYVE recycling and an increasing chance that the fusion protein is sorted into ILVs. On the other hand, if the ESCRT-III binding affinity of the MIT domain drops too low, the sorting efficiency drops and the fusion protein will behave more like GFP-FYVE, a non-interacting protein. This effect could explain why MIT(L64D)-GFP-FYVE was found to be a better cargo than MIT(I18D,L64D)-GFP-FYVE. In summary, the data supported the notion that, depending on the interaction strength, binding to ESCRT-III resulted either in MVB sorting (weak interaction) or recycling from the endosome (strong interaction).

We analyzed the localization of the remaining ESCRT-III interacting GFP-FYVE constructs. The domains tested were the N-terminal region of Bro1 (Bro1 domain), the C-terminal catalytic domain of the deubiquitinating enzyme Doa4 (localizes via Bro1 to ESCRT-III) and the N-terminal region of Did2 (31, 32).

Both Bro1(N)-GFP-FYVE and Doa4(C)-GFP-FYVE were efficiently sorted into the lumen of the vacuole and thus mimicked cargo proteins (Figure 3C). When expressed in strains containing either a mutant *RSP5* allele (*rsp5-1*) or the deubiquitinating Hse1-DUB protein the GFP signal of both Bro1(N)-GFP-FYVE and Doa4(C)-GFP-FYVE localized mainly to the lumen of the vacuole, indicating that MVB sorting of these proteins was ubiquitin-independent (Figure 3D). In contrast, the delivery to the vacuolar lumen was dependent on functioning ESCRT machinery (*vps43*Δ, Figure 3D). Mutating the Bro1-binding site in Doa4(C)-GFP-FYVE (33) blocked delivery of the fusion protein into the vacuolar lumen (Doa4(C,AAFA)-GFP-FYVE, Figure 3C), further demonstrating that MVB sorting of Doa4(C)-GFP-FYVE is independent of ubiquitination but requires binding to ESCRT-III via Bro1.

The localization of Did2(N)-GFP-FYVE mimicked ESCRT machinery (Figures 3C), suggesting that this ESCRT-III binding protein was removed from the MVB prior to fusion with the vacuole. One explanation for the efficient recycling of the fusion protein could be a strong interaction of the Did2(N) domain to ESCRT-III, thus mimicking the behavior of MIT-GFP-FYVE.

Together, the data of GFP-FYVE fusions indicated that strong binding to ESCRT-III could indeed result in a protein mimicking ESCRT machinery. The recycling of these fusion proteins from the MVB was most likely mediated by the Vps4-dependent disassembly of ESCRT-III. Not expected was the observation that weaker interactions with ESCRT-III would cause sorting of the fusion protein into ILVs. This result was particularly surprising considering that ESCRT-III has been postulated to function late in the formation of ILVs, mainly acting together with Vps4 in the membrane fission reaction that releases the forming vesicles into the lumen of the MVB (Figure 1A).

Binding to the early ESCRT machinery mediates MVB sorting

We tested two ESCRT-mimics that were designed to bind to the early ESCRT machinery (Figure 1A). The first fusion protein contained the PSDP domain, the region of Vps27 that has been shown to interact with ESCRT-I (34). The second construct contained the C-terminal region of Vps28, the region of ESCRT-I that is known to bind to ESCRT-II (35). Both of these constructs, Vps27(PSDP)-GFP-FYVE and Vps28(C)-GFP-FYVE, did not recycle to the cytoplasm but instead sorted into the MVB pathway. The sorting efficiency was rather low, suggesting that these fusion proteins behaved as poor MVB cargo (Figure 4A). Mutating *RSP5* or expressing *HSE1-DUB* had weak or no effects on the sorting of these fusion proteins, indicating that they entered the MVB pathway in a ubiquitin-

independent manner (Figure 4B). However, Vps4, and thus ESCRT activity, was necessary for the delivery of the fusion protein to the vacuolar lumen (Figure 4B).

To compare the sorting efficiency of Vps27(PSDP)-GFP-FYVE and Vps28(C)-GFP-FYVE with that of a corresponding ubiquitinated cargo, a fusion protein of ubiquitin and GFP-FYVE was constructed. Surprisingly, when expressed in yeast, Ub-GFP-FYVE localized to endosomes and the vacuolar membrane, indicating that this fusion protein was not recognized by the ESCRT machinery as ubiquitinated cargo but, in contrast, mimicked a non-interacting protein (data not shown). One explanation for this result might be that the ubiquitin domain of Ub-GFP-FYVE was inaccessible to the ESCRTs. Therefore, a fusion protein was constructed that contained a second ubiquitin domain at the membrane-proximal C-terminus of the fusion protein. The resulting 2Ub-GFP-FYVE fusion was partially sorted into the lumen of the vacuole, mimicking the sorting of poor MVB cargo (Figure 4A). The poor sorting of 2Ub-GFP-FYVE, Vps27(PSDP)-GFP-FYVE and Vps28(C)-GFP-FYVE was not the result of proteolytic clipping of the EID in the cytosol since western blot analysis showed that the majority of the fusion proteins present in a *vps4*Δ strain were full length (the strain contained additional deletions of vacuolar peptidases to minimize proteolysis during sample preparation, Figure 4C). Together, the data suggested that the ESCRT-I and ESCRT-II binding domains used (Vps27(PSDP) and Vps28(C)) acted as MVB sorting signals that were as efficient as ubiquitin itself.

MVB sorting is independent of the type of membrane association

To determine if the type of membrane association plays a role in the ubiquitin-independent sorting of cargo into the MVB pathway, we fused the MIT and Vps28(C) domains to the N-terminus of the type II-transmembrane protein GFP-Dap2 (Figure 1B and Table 1). We observed that both the ESCRT-III binding domain (MIT) and the ESCRT-II binding domain (Vps28(C)) caused sorting of the corresponding fusion proteins into the lumen of the vacuole (Figure 4D). Unlike MIT-GFP-FYVE, which is recycled together with the ESCRT machinery, MIT-GFP-Dap2 is a transmembrane protein that cannot be removed from the MVB and thus is efficiently packaged into ILVs. The MVB sorting of these fusion proteins was mainly independent of ubiquitination, since mutating *RSP5* (*rsp5-1* strain) or expressing *HSE1-DUB* caused only minor drop in the localization to the vacuolar lumen (Figure 4D). The MVB sorting of MIT-GFP-Dap2 was more efficient than sorting of Vps28(C)-GFP-Dap2, a fusion protein that showed partial vacuolar membrane localization (Figure 4D). The poor sorting of Vps28(C)-GFP-Dap2 was not caused by proteolytic clipping of the fusion proteins since western blot analysis showed that the majority of the fusion proteins present in a *vps4*Δ strain were full length (Figure 4E). This observation was consistent with the data obtained from the GFP-FYVE fusions, demonstrating more efficient MVB sorting of ESCRT-III-binding proteins compared to early ESCRT-binding proteins. Together, these experiments indicated that, independent of the type of membrane association, binding to ESCRT-II or ECSRT-III could serve as an ubiquitin-independent sorting signal for the MVB pathway. However, previous studies have shown that the fusion protein MIT-GFP does not localize to the vacuole (28), indicating that ESCRT binding alone is not sufficient for MVB sorting. Therefore we conclude that membrane association is necessary in order for a protein to be sorted into ILVs.

In silico analysis of the MVB sorting model

Previous models of ESCRT function suggested that the ESCRTs assemble into a temporally and spatially highly ordered structure in which cargo is sorted by the early ESCRTs (ESCRT-0, -I, -II) and membrane deformation and membrane fission is executed by ESCRT-III and Vps4 function (Figure 1A). In contrast, our data suggested that all the ESCRTs are able to mediate cargo sorting and we found that a simple change in ESCRT

affinity converted a protein that behaved like an ESCRT component to a protein that was efficiently sorted into ILVs. The ESCRT mimics contained ESCRT-interaction domains that compete with endogenous ESCRTs for binding to the ESCRT network. Even though the mimics were expressed at higher levels than the endogenous ESCRTs (based on GFP signals) they did not interfere with normal ESCRT function (Table 2). Similarly, the fusion proteins that behaved like cargoes were binding to sites of the ESCRT machinery that normally are not interacting with cargo.

To explain our data we propose a model in which cargoes trigger the assembly of ESCRTs on the endosomal membrane into a protein network with great flexibility. Although each of the ESCRT complexes has a defined quarternary structure with defined interaction sites, the position of the ESCRTs within the network is not fixed and each particular position can be occupied by either machinery or cargo. A simplified view of this model would be a system of just two different components, cargo and ESCRT, that polymerize together into a 2D-lattice. The question remains if such a simple system would be able to specifically sort cargo and leave non-cargo (or non-interacting proteins) behind. To answer this question we turned to computer modeling. For the *in silico* model we used a two-dimensional hexagonal grid to represent the membrane surface on which membrane-associated proteins were able to randomly move and interact. The sorting simulation contained three types of elements: 1) ESCRTs containing one cargo-binding site and 5 ESCRT-ESCRT interaction sites, 2) cargoes and 3) non-cargoes (not to be sorted by the system). The starting condition was a random distribution of specified proportions of cargoes and non-cargoes. Binding and movement of proteins were randomly determined based on probabilities (described in more detail in Materials and Methods). The goal of the simulation was to test the hypotheses that the protein interactions were sufficient to achieve high ESCRT-dependent sorting efficiency and fidelity, namely that all cargoes should be sorted into vesicles whereas all non-cargoes should be excluded.

A simplified example of the cargo sorting simulation is shown in Figure 5. The basic rules for the computer model are as follows. 1) ESCRTs are recruited to the membrane from the cytoplasm by binding to cargo (appear next to a cargo on the grid), diffuse on the grid together with the bound cargo, can bind to other ESCRTs, or can break the interaction with cargo which releases the ESCRT into the cytoplasm. We assume that ESCRTs are not stable on the membrane without interacting with other proteins and therefore are removed from the membrane if unbound (disappear from the grid). 2) All proteins and protein complexes can diffuse on the membrane and form new interactions with each other (ESCRT can bind one cargo and up to 5 ESCRTs) 3) ESCRT-cargo and ESCRT-ESCRT interactions can break. However, a network of more than two proteins (ESCRT or cargo) is stable and cannot break. 4) Networks and their bound cargoes and entrapped non-cargoes are removed from the grid (simulating vesicle formation) with probability depending on the size of the network.

We found that stabilization of the ESCRTs by multiple interactions (ESCRT-cargo or ESCRT-ESCRT interactions, rules 1 and 3) was important to form larger networks and to prevent ESCRTs alone to form networks. This rule is consistent with recent data demonstrating the necessity of ubiquitinated cargo for ESCRT function (30). Running the computer simulation starting with different conditions found that sorting efficiency and fidelity was very high and not dependent on the concentration of cargo or non-cargo (Figures 6A and 6B, Movie S1). Only rarely non-cargo became entrapped by the ESCRT-cargo network and was removed during the vesicle formation step of the simulation. Furthermore, including a component with a single ESCRT-interaction site to the starting conditions, a component that mimicked the behavior of a GFP-FYVE fusion construct, did not disrupt the formation of networks and resulted in efficient sorting of both cargo and the GFP-FYVE mimic (Figure 6A). Furthermore, changing the number of ESCRT-ESCRT

interaction sites of the ESCRT components from 5 to 4 or 3 did not diminish sorting efficiency and fidelity (Figure 6A). Together, the simulations showed that the proposed cargo-sorting system is robust and highly adaptable to various conditions.

Discussion

Our study provided key insight into the rules that govern ESCRT recycling and MVB cargo sorting. The key conclusions are:

Cargo sorting can be mediated by binding to any ESCRT complex

Our data suggested that binding to ESCRT-I, ESCRT-II or ESCRT-III leads to sorting into the MVB pathway. This observation is unexpected because previous models, such as the epistasis model shown in Figure 1A suggested that cargo sorting is mediated mainly by the 'early ESCRTs' (ESCRT-0, ESCRT-I, ESCRT-II) whereas ESCRT-III and Vps4 function only in ILV formation.

ESCRT-III and Vps4 function concurrently with cargo sorting

ESCRT-III and Vps4 have been predicted to act solely as membrane fission machinery, severing the membrane neck after cargo sorting and membrane deformation has been completed. In contrast, our data indicated that ESCRT-III can participate in cargo sorting, suggesting that ESCRT-III assembles before a narrow neck inhibits diffusion of cargo in and out of the forming ILV. Furthermore, the fate of the MIT-GFP-FYVE depended on its interaction strength with ESCRT-III, suggesting that Vps4 mediated disassembly of ESCRT-III is concurrent with cargo sorting.

Cargo ubiquitination is not required for sorting into the MVB pathway

Every ESCRT-interaction domain we tested was able to function as a MVB sorting signal, suggesting that ubiquitin is not a unique sorting signal that is essential for entry into the ILV. Rather, our data suggested that ubiquitin functions as temporary ESCRT-interaction domain that can be added and removed from proteins in order to regulate their interaction with the ESCRT machinery. Recent studies showed that aquaporin AQP2 and the G protein-coupled receptor PAR1 are sorted into the MVB pathway independent of ubiquitination (36, 37). In both cases, MVB sorting was mediated by direct interactions with ESCRT factors that are predicted to function together with ESCRT-III and Vps4 at later stages of ILV formation (LIP5 and ALIX). These studies are consistent with our findings that direct interaction with ESCRT-III or ESCRT-III-associated proteins can result in efficient delivery to the vacuolar lumen.

Soluble proteins can be sorted into the MVB pathway

A few examples of soluble MVB cargo have been described in the literature. However, it is not understood how these proteins are delivered into forming ILVs whereas all the other cytoplasmic proteins are excluded. Published examples include MVB-dependent degradation of soluble signaling proteins (38, 39) and the packaging of soluble proteins into exosomal vesicles (40), an ESCRT-mediated process similar to MVB cargo sorting. We conclude from our studies that soluble proteins can be sorted into the MVB pathway but membrane-association is essential for this process. Similar to transmembrane proteins, binding to any ESCRT component seems to serve as a sorting signal for soluble proteins. However, the interaction strength between soluble cargo and ESCRTs must be weak, otherwise the cargo protein will be removed together with the ESCRTs from the MVB and recycled back to the cytoplasm.

ESCRTs and their cargoes are alike

ESCRTs are endosome-associated proteins that interact with other ESCRTs and are modified by ubiquitination (17). Why then are ESCRTs not efficient cargoes? This question was answered by the analysis of MIT-GFP-FYVE. This ESCRT-III-interacting fusion protein cycled between MVBs and cytoplasm and thus resembled the localization of an ESCRT protein. However, mutating one of the ESCRT-III binding sites of the MIT domain converted the fusion protein into an efficient MVB cargo (MIT(L64D)-GFP-FYVE, Figure 3). This result suggested that a weak interaction with the ESCRT machinery resulted in efficient sorting into the MVB pathway, whereas a strong affinity to the ESCRTs was essential to promote recycling to the cytoplasm. Therefore, the key event that determines the fate of an MVB-associated protein seems to be the competition between the interaction of the protein with the membrane and ESCRT machinery: if the membrane-interaction wins, the protein becomes a cargo, if it loses, the protein is recycled and behaves like an ESCRT protein. Because transmembrane proteins are thoroughly anchored in the membrane, the membrane-interaction always wins this competition and thus even strongly ESCRT-interacting proteins are efficiently sorted into the MVB pathway (e.g. MIT-GFP-Dap2, Figure 4D).

The protein network formed by early ESCRTs shows a high degree of variability and built-in redundancy

Two of the fusion proteins we constructed are sorted into the MVB pathway by binding to the ESCRT-0 – ESCRT-I and the ESCRT-I – ESCRT-II interactions sites. Surprisingly, the presence of these fusion proteins did not interfere with ESCRT function (Table 2), even though these proteins were competing with ESCRTs for the same interaction sites and were expressed at higher levels than the ESCRTs. For example, Vps28(C)-GFP-FYVE is predicted to compete with ESCRT-I for the interaction with ESCRT-II, however, no dominant-negative effect was observed. Furthermore, Vps28(C)-GFP-FYVE is sorted like a cargo even though it occupies the space in the ESCRT network that is normally reserved for ESCRT-I. Together, these observations support a model in which ESCRT-0, ESCRT-I and ESCRT-II assemble into a network that can adapt to various cargoes by changing the local structure. Furthermore, this system shows a high degree of redundancy; disruption of some of the ESCRT-ESCRT interactions does not impair the cargo sorting mechanism. Consistent with this model, we found no particular entry point for cargo into the ESCRT system. Even interaction with ESCRT-III, a complex thought to mainly act in the final membrane fission step of MVB vesicle formation, mediated efficient cargo sorting. Therefore, we found no evidence for a strict temporal order within the ESCRT system (as depicted in Figure 1A) that would limit the cargo sorting function to only the early ESCRTs. Similarly, no single ubiquitin-binding site of the ESCRT machinery was found to be essential for cargo sorting (41).

Together our data can be explained with a simple oligomerization model in which the ESCRTs together with membrane-associated ESCRT-binding proteins co-assemble on the endosomal membrane (Figure 7). For the purpose of cargo sorting, the identity of the ESCRT complex binding to the cargo and the type of interaction (ubiquitin-dependent or not) seems to be irrelevant. The resulting protein network defines the area on the endosomal membrane that will form an ILV. Non-interacting proteins (or non-cargoes) are excluded from this area simply by steric hindrance. *In silico* studies showed that such a simple system is able to efficiently sort cargoes (Figure 6). The final structure and composition of the protein network is not defined but adapts to the size and structure of the components. However, it is likely that the ESCRT system has an overall organization. This order within the ESCRT system might be provided by ESCRT-III, a spiral-forming polymer that could act as the ‘backbone’ of the network, giving the ESCRT system directionality. After the

oligomerization reaction, the vesicle formation phase is initiated by the disassembly of the protein network by Vps4 and the deubiquitinating enzyme Doa4. This stage decides which components of the network will behave like ESCRT machinery and which components will become cargoes of the MVB pathway. ESCRT components are recycled whereas cargoes remain associated with a membrane region that invaginates by a lipid-driven mechanism and forms the ILV (discussed in (42). In a final step, ESCRT-III and Vps4 are likely to drive the membrane fission reaction that completes the ILV formation.

Materials and Methods

Strains, media and plasmids

The strains and plasmids used in this study are described in Table 2. Yeast Gene knockouts were constructed as previously described (43). Plasmids were constructed using conventional restriction enzymes or by Quikchange mutagenesis protocol using Phusion polymerase enzyme. pSK11 and pSD2 were constructed by inserting the previously described GFP-Dap2 and GFP-Cps1 constructs, respectively (25, 44), into pRS415 vector. Similar vector swap was performed for the previously published GFP-FYVE construct (14) to obtain pSK43. pSK122 was constructed by fusing the ubiquitination sequence from Cps1 to the N-terminus of GFP-Dap2. Yeast strains were grown in rich YPD (yeast extract-peptone-dextrose) medium or in the appropriate synthetic drop out media (YNB) as published (45). In every set of microscopy experiments, strains were grown in the same growth medium. 100μM $CuSO_4$ was added to the medium to drive the expression of *CUP1* promoter containing constructs.

Western blot analysis

Yeast cell extracts for western blotting were obtained from strains grown to logarithmic phase. Cells were pelleted, resuspended in SDS-PAGE sample buffer (2% SDS, 0.1M Tris pH6.8, 10% Glycerol, 0.01% bromophenol blue, 5% β-mercaptoethanol) and lysed using glass beads. The anti-GFP antibody used in western blotting was purchased from Roche Diagnostics Corporation (Indianapolis, IN). The anti-Snf7 antibody used was previously described (46).

Fluorescence microscopy and quantification

Yeast strains were grown for 10–14 hours in YNB to optical densities of 0.7 (at 600nm). 100μM $CuSO_4$ was added 3.5 hours before microscopy analysis to cells containing *CUP1* promoter driven constructs. Fluorescence microscopy was performed on a deconvolution microscope (DeltaVision, Applied Precision, Issaquah, WA). 50 cells of each strain were used to determine point-values for the vacuolar limiting membrane, the vacuolar lumen and the endosome. Because of its small size the endosomal values were defined as the brightest pixel of the endosomal structure. The value for the vacuolar lumen was determined by calculating the average intensity of 150 pixels within the vacuole. Similarly, the value for the vacuolar membrane was determined by averaging the intensities of 50 pixels representing the limiting membrane of the vacuole. The background value was measured as the average of 150 pixels outside of and in close proximity to each cell. The background value was subtracted from each of the above measurements resulting in the values for endosome, vacuolar lumen and vacuolar membrane (see Figure 1C). In cells with efficient MVB cargo sorting, the vacuolar membrane was not clearly visible. In such cases, vacuolar membrane was given the same value as vacuolar lumen. In cells with multiple vacuoles, the most prominent vacuole was used for quantification. Cutoff values were defined to exclude cells with very high (causing sorting defects) or very low (low signal-to-noise ratio) fluorescence intensities from the analyses.

Invertase assay

The liquid invertase assay was performed as previously described (47). Strains were grown in YNB medium to a density of 0.6–0.9 OD_{600}. 0.5 ODV of each strain was washed with and resuspended in 1ml 0.1 M sodium acetate (pH 4.9). A 50 μl aliquot of each yeast suspension was incubated with 12.5 μl of 1 M sucrose at 30 °C for 30 minutes. Simultaneously, glucose standards solutions containing 0, 0.4, 0.8, 1.2 and 1.6 mM glucose were made in 50 μl NaAc and incubated with 12.5 μl of 1 M sucrose. Reactions were quenched by adding 75 μl of 0.2 M dipotassium phosphate solution and placed on ice. 500 μl of Glucostat reagent (2.5 μg/ml horseradish peroxidase, 2 units/ml Glucose oxidase, 100 μM *N*-Ethylmaleimide, 614 μM *o*-Dianisidine in 0.1 M dipotassium phosphate buffer (pH 7)) was added to each of the aliquots and incubated at 30 °C for 30 min. Reactions were stopped with 500 μl of 6 M hydrochloric acid and OD_{540} was measured for each sample. All samples were done in triplicates. The averaged value for each strain was normalized with the negative control (BHY10 strain containing empty vector) at 0 % and positive control (BHY10 strain containing $vps4^{E233Q}$) at 100 %.

Computer Simulations

MATLAB was used to run all computer simulations. A cellular automata model was employed on a two-dimensional hexagonal grid. The grid size used in all simulations is 28 by 28. The simulation involves randomly selecting grid points and updating the grid according to a given set of rules for assigning probabilities of updates according to the current state of the grid. Inputs to the simulation include: 1) initial proportions of cargo, non-cargo, and GFP-FYVE construct in the grid, 2) number of ESCRT - ESCRT binding sites, 3) parameters specifying propensities for diffusion, ESCRT - ESCRT binding, ESCRT -cargo binding, ESCRT - GFP-FYVE binding, ESCRT removal, unbinding, and critical vesicle size.

Every protein in the grid is associated with a network which includes all the proteins it is connected to through bonds. An unbound protein is simply considered a network of one protein. As proteins bind together, larger networks are formed. Updates may affect the entire network of the grid point selected and not just the individual grid point selected to update. Potential updates are determined by the following rules for each type of update.

Recruitment of ESCRTs—ESCRTs will be recruited to an empty grid point if there is at least one cargo in an adjacent grid point. The recruited ESCRT is bound to an adjacent cargo.

Removal of ESCRTs—Unbound ESCRTs may be removed from the grid. Upon removal, the current grid point becomes empty. Due to our choice of parameters, it is almost certain that an unbound ESCRT will be removed from the grid.

Binding—The hexagonal grid allows for up to six bindings per protein. However, cargo and GFP-FYVE are limited to one binding. ESCRTs have one cargo binding site and up to five ESCRT binding sites. The number of allowed ESCRT binding sites is specified as an input. If GFP-FYVE is present in the simulation, it may occupy one of the ESCRT binding sites of an ESCRT. Cargo may bind to one ESCRT. GFP-FYVE may bind to one ESCRT. ESCRTs may bind to one cargo, one GFP-FYVE (if present), and up to five other ESCRTS.

Unbinding—Cargo may only unbind if its network is an ESCRT – cargo pair. If a cargo is part of a network of three or more proteins, the cargo is prohibited from unbinding. An ESCRT may unbind from if it has only a single bond with another ESCRT and no other interactions. GFP-FYVE is prohibited from unbinding once it is bound to an ESCRT.

Diffusion—Networks of any size are allowed to move in any of six directions (up left, down right, up right, down left, left, right) if all of the adjacent grid spaces to the network in that direction are empty. If any adjacent space is occupied by a protein, including adjacent spaces in the interior of the network, movement of the network is prohibited.

Rotation—Any protein bound to only one other protein is allowed to rotate clockwise if the adjacent grid space in the clockwise direction is empty. Similarly, a protein bound to only one other protein is allowed to rotate in the counter-clockwise direction as well.

Removal of networks and trapped non-cargoes—As networks grow they may be removed from the system mimicking vesicle formation. An input to the simulation is critical vesicle size, which is defined as a sufficient number of proteins included in a network in order to form a vesicle. We calculate the value $V(N) = 1/(1+\exp(-(N-C)))$ where N is the size of the current network defined by the number of proteins in the network and C is the critical vesicle size. As a function of N, V is a sigmoid function centered at C. If the computed value of V is greater than a randomly generated number, the entire network is removed from the grid and every grid point occupied by the network becomes empty. As a network grows it is more likely to be removed from the grid as V is an increasing function. A network rarely grows much larger than the critical vesicle size due to the nature of V(N). In addition, small networks are almost never removed from the grid. It is possible that non-cargo may be trapped in a network which is selected to be removed from the grid. A non-cargo is considered trapped if 1) it is in an interior row of the current network and 2) in each interior row of the network, it is in an interior column of that row. If a non-cargo is trapped when a network is removed, it is also removed with the network and the grid point occupied by that non-cargo becomes empty. This is the only way that non-cargo can be removed from the grid.

Determination of probabilities—The probability of each allowable update for a selected non-empty grid point is determined by the propensity for that update scaled by the sum of propensities for all allowable updates. Therefore, the probabilities of all possible updates sum to one. Further, if only one update is allowable, that update will be selected with probability one. If an empty grid point is selected, an ESCRT will be recruited with probability one if at least one cargo occupies an adjacent grid point. Otherwise, the empty grid space remains empty.

Simulation—To begin each simulation, a random grid is generated based on the initial proportions of cargo, non-cargo, and GFP-FYVE specified. Following the initial grid setup, the simulation repeats as follows until a specified number of runs are completed. Updates to the grid are selected based on the calculated probabilities.

1. Randomly select a grid point.
2. Determine the occupancy type of all the grid points adjacent to the current grid point.
3. Is the current grid point empty?
    - Yes: Move to step 4.
    - No: Move to step 5.
4. Recruit an ESCRT?
    - Yes: Add an ESCRT to the current grid point, bind the ESCRT to an adjacent cargo, and begin again with step 1.

- No: Begin again with step 1.

5. Remove network of current grid point?
    - Yes: Remove network (along with any trapped non-cargo) and begin again with step 1.
    - No: Move to step 6.
6. Determine what updates are possible for the current grid point or the network of the current grid point.
7. Is there at least one possible update?
    - Yes: Randomly select one of the possible updates and update the grid. Begin again with step 1.
    - No: Begin again with step 1.

While initial proportions and number of ESCRT -ESCRT bindings varied for the results shown, the propensity parameters used for all simulations are as follows:

Diffusion (for all proteins): 1,

ESCRT – ESCRT binding: 10,

ESCRT – Cargo binding: 10,

ESCRT – GFP-Fyve binding: 10,

ESCRT Removal: 1000,

Unbinding: 1, and

Critical Vesicle Size: 20.

We set the propensity parameters for binding to be equal, independent of protein type. However, since the updates are determined by the calculated probabilities, an ESCRT (with 5 ESCRT – ESCRT interaction sites) is usually more likely to associate with another ESCRT than a cargo since it has 5 ESCRT interaction sites and only one cargo interaction site. In this type of probability driven model, binding affinities are not explicitly specified, rather, the qualitative behavior of the protein interactions were accounted for.

For each set of initial proportions of proteins 20 simulations were completed. The amounts of each type of protein (cargo, non-cargo, ESCRT, and GFP-FYVE) were recorded at 100 intervals of 2500 steps of each simulation. The data from each simulation were normalized by dividing by the total number of grid spaces (in this case 28^2) giving a grid concentration of each protein type. The average and standard deviation of the 20 simulations were calculated. Movie frames were captured every 250 runs of a simulation and include 700 frames. Furthermore, still images of the same simulation were recorded.

Supplementary Material

Refer to Web version on PubMed Central for supplementary material.

Acknowledgments

We thank Rob Piper for sharing plasmids and for helpful discussions. This work has been supported by grants NIH R01 GM074171 (to M.B.) and NSF-DMS 1122297 (to J.P.K.).

Abbreviations

ESCRT	endosomal sorting complex required for transport
ILV	intraluminal vesicle
MVB	multivesicular body
PI-3P	phosphatidylinositol-3-phosphate

References

1. Henne WM, Buchkovich NJ, Emr SD. The ESCRT pathway. Dev Cell. 2011; 21(1):77–91. [PubMed: 21763610]
2. Shields SB, Piper RC. How ubiquitin functions with ESCRTs. Traffic. 2011; 12(10):1306–1317. [PubMed: 21722280]
3. Hurley JH. The ESCRT complexes. Crit Rev Biochem Mol Biol. 2010; 45(6):463–487. [PubMed: 20653365]
4. Babst M. A protein's final ESCRT. Traffic. 2005; 6(1):2–9. [PubMed: 15569240]
5. Muziol T, Pineda-Molina E, Ravelli RB, Zamborlini A, Usami Y, Gottlinger H, Weissenhorn W. Structural basis for budding by the ESCRT-III factor CHMP3. Dev Cell. 2006; 10(6):821–830. [PubMed: 16740483]
6. Hanson PI, Roth R, Lin Y, Heuser JE. Plasma membrane deformation by circular arrays of ESCRT-III protein filaments. J Cell Biol. 2008; 180(2):389–402. [PubMed: 18209100]
7. Bajorek M, Schubert HL, McCullough J, Langelier C, Eckert DM, Stubblefield WM, Uter NT, Myszka DG, Hill CP, Sundquist WI. Structural basis for ESCRT-III protein autoinhibition. Nat Struct Mol Biol. 2009; 16(7):754–762. [PubMed: 19525971]
8. Xiao J, Chen XW, Davies BA, Saltiel AR, Katzmann DJ, Xu Z. Structural basis of Ist1 function and Ist1-Did2 interaction in the multivesicular body pathway and cytokinesis. Mol Biol Cell. 2009; 20(15):3514–3524. [PubMed: 19477918]
9. Bodon G, Chassefeyre R, Pernet-Gallay K, Martinelli N, Effantin G, Hulsik DL, Belly A, Goldberg Y, Chatellard-Causse C, Blot B, Schoehn G, Weissenhorn W, Sadoul R. Charged multivesicular body protein 2B (CHMP2B) of the endosomal sorting complex required for transport-III (ESCRT-III) polymerizes into helical structures deforming the plasma membrane. J Biol Chem. 2011; 286(46):40276–40286. [PubMed: 21926173]
10. Hurley JH, Hanson PI. Membrane budding and scission by the ESCRT machinery: it's all in the neck. Nat Rev Mol Cell Biol. 2010; 11(8):556–566. [PubMed: 20588296]
11. Wurmser AE, Emr SD. Phosphoinositide signaling and turnover: PtdIns(3)P, a regulator of membrane traffic, is transported to the vacuole and degraded by a process that requires lumenal vacuolar hydrolase activities. Embo J. 1998; 17(17):4930–4942. [PubMed: 9724630]
12. Katzmann DJ, Stefan CJ, Babst M, Emr SD. Vps27 recruits ESCRT machinery to endosomes during MVB sorting. J Cell Biol. 2003; 162(3):413–423. [PubMed: 12900393]
13. Misra S, Hurley JH. Crystal structure of a phosphatidylinositol 3-phosphate-specific membrane-targeting motif, the FYVE domain of Vps27p. Cell. 1999; 97(5):657–666. [PubMed: 10367894]
14. Burd CG, Emr SD. Phosphatidylinositol(3)-phosphate signaling mediated by specific binding to RING FYVE domains. Mol Cell. 1998; 2(1):157–162. [PubMed: 9702203]
15. Gaullier JM, Simonsen A, D'Arrigo A, Bremnes B, Stenmark H, Aasland R. FYVE fingers bind PtdIns(3)P [letter; comment]. Nature. 1998; 394(6692):432–433. [PubMed: 9697764]
16. Stringer DK, Piper RC. A single ubiquitin is sufficient for cargo protein entry into MVBs in the absence of ESCRT ubiquitination. J Cell Biol. 2011; 192(2):229–242. [PubMed: 21242292]
17. Erpapazoglou Z, Dhaoui M, Pantazopoulou M, Giordano F, Mari M, Leon S, Raposo G, Reggiori F, Haguenauer-Tsapis R. A dual role for K63-linked ubiquitin chains in multivesicular body biogenesis and cargo sorting. Mol Biol Cell. 2012; 23(11):2170–2183. [PubMed: 22493318]

18. Malerod L, Pedersen NM, Sem Wegner CE, Lobert VH, Leithe E, Brech A, Rivedal E, Liestol K, Stenmark H. Cargo-dependent degradation of ESCRT-I as a feedback mechanism to modulate endosomal sorting. Traffic. 2011; 12(9):1211–1226. [PubMed: 21564451]
19. Wang Z, Hill S, Luther JM, Hachey DL, Schey KL. Proteomic analysis of urine exosomes by multidimensional protein identification technology (MudPIT). Proteomics. 2012; 12(2):329–338. [PubMed: 22106071]
20. Curtiss M, Jones C, Babst M. Efficient cargo sorting by ESCRT-I and the subsequent release of ESCRT-I from multivesicular bodies requires the subunit Mvb12. Mol Biol Cell. 2007; 18(2):636–645. [PubMed: 17135292]
21. Stenmark H, Aasland R, Toh BH, D'Arrigo A. Endosomal localization of the autoantigen EEA1 is mediated by a zinc- binding FYVE finger. J Biol Chem. 1996; 271(39):24048–24054. [PubMed: 8798641]
22. Raiborg C, Bremnes B, Mehlum A, Gillooly DJ, D'Arrigo A, Stang E, Stenmark H. FYVE and coiled-coil domains determine the specific localisation of Hrs to early endosomes. J Cell Sci. 2001; 114(Pt 12):2255–2263. [PubMed: 11493665]
23. Kutateladze TG, Ogburn KD, Watson WT, de Beer T, Emr SD, Burd CG, Overduin M. Phosphatidylinositol 3-phosphate recognition by the FYVE domain. Mol Cell. 1999; 3(6):805–811. [PubMed: 10394369]
24. Roberts CJ, Pohlig G, Rothman JH, Stevens TH. Structure, biosynthesis, and localization of dipeptidyl aminopeptidase B, an integral membrane glycoprotein of the yeast vacuole. J Cell Biol. 1989; 108(4):1363–1373. [PubMed: 2647766]
25. Odorizzi G, Babst M, Emr SD. Fab1p PtdIns(3)P 5-kinase function essential for protein sorting in the multivesicular body. Cell. 1998; 95(6):847–858. [PubMed: 9865702]
26. Dimaano C, Jones CB, Hanono A, Curtiss M, Babst M. Ist1 regulates vps4 localization and assembly. Mol Biol Cell. 2008; 19(2):465–474. [PubMed: 18032582]
27. Kieffer C, Skalicky JJ, Morita E, De Domenico I, Ward DM, Kaplan J, Sundquist WI. Two distinct modes of ESCRT-III recognition are required for VPS4 functions in lysosomal protein targeting and HIV-1 budding. Dev Cell. 2008; 15(1):62–73. [PubMed: 18606141]
28. Shestakova A, Hanono A, Drosner S, Curtiss M, Davies BA, Katzmann DJ, Babst M. Assembly of the AAA ATPase Vps4 on ESCRT-III. Mol Biol Cell. 2010
29. Wang G, Yang J, Huibregtse JM. Functional domains of the Rsp5 ubiquitin-protein ligase. Mol Cell Biol. 1999; 19(1):342–352. [PubMed: 9858558]
30. MacDonald C, Buchkovich NJ, Stringer DK, Emr SD, Piper RC. Cargo ubiquitination is essential for multivesicular body intralumenal vesicle formation. EMBO Rep. 2012; 13(4):331–338. [PubMed: 22370727]
31. Luhtala N, Odorizzi G. Bro1 coordinates deubiquitination in the multivesicular body pathway by recruiting Doa4 to endosomes. J Cell Biol. 2004; 166(5):717–729. [PubMed: 15326198]
32. Nickerson DP, West M, Odorizzi G. Did2 coordinates Vps4-mediated dissociation of ESCRT-III from endosomes. J Cell Biol. 2006; 175(5):715–720. [PubMed: 17130288]
33. Richter C, West M, Odorizzi G. Dual mechanisms specify Doa4-mediated deubiquitination at multivesicular bodies. EMBO J. 2007; 26(10):2454–2464. [PubMed: 17446860]
34. Bilodeau PS, Winistorfer SC, Kearney WR, Robertson AD, Piper RC. Vps27-Hse1 and ESCRT-I complexes cooperate to increase efficiency of sorting ubiquitinated proteins at the endosome. J Cell Biol. 2003; 163(2):237–243. [PubMed: 14581452]
35. Gill DJ, Teo H, Sun J, Perisic O, Veprintsev DB, Emr SD, Williams RL. Structural insight into the ESCRT-I/-II link and its role in MVB trafficking. EMBO J. 2007; 26(2):600–612. [PubMed: 17215868]
36. van Balkom BW, Boone M, Hendriks G, Kamsteeg EJ, Robben JH, Stronks HC, van der Voorde A, van Herp F, van der Sluijs P, Deen PM. LIP5 interacts with aquaporin 2 and facilitates its lysosomal degradation. Journal of the American Society of Nephrology: JASN. 2009; 20(5):990–1001. [PubMed: 19357255]
37. Dores MR, Chen B, Lin H, Soh UJ, Paing MM, Montagne WA, Meerloo T, Trejo J. ALIX binds a YPX(3)L motif of the GPCR PAR1 and mediates ubiquitin-independent ESCRT-III/MVB sorting. J Cell Biol. 2012; 197(3):407–419. [PubMed: 22547407]

38. Ikeda H, Kerppola TK. Lysosomal localization of ubiquitinated Jun requires multiple determinants in a lysine-27-linked polyubiquitin conjugate. Mol Biol Cell. 2008; 19(11):4588–4601. [PubMed: 18716056]
39. Taelman VF, Dobrowolski R, Plouhinec JL, Fuentealba LC, Vorwald PP, Gumper I, Sabatini DD, De Robertis EM. Wnt signaling requires sequestration of glycogen synthase kinase 3 inside multivesicular endosomes. Cell. 2010; 143(7):1136–1148. [PubMed: 21183076]
40. Gibbings DJ, Ciaudo C, Erhardt M, Voinnet O. Multivesicular bodies associate with components of miRNA effector complexes and modulate miRNA activity. Nat Cell Biol. 2009; 11(9):1143–1149. [PubMed: 19684575]
41. Shields SB, Oestreich AJ, Winistorfer S, Nguyen D, Payne JA, Katzmann DJ, Piper R. ESCRT ubiquitin-binding domains function cooperatively during MVB cargo sorting. J Cell Biol. 2009; 185(2):213–224. [PubMed: 19380877]
42. Babst M. MVB vesicle formation: ESCRT-dependent, ESCRT-independent and everything in between. Curr Opin Cell Biol. 2011; 23(4):452–457. [PubMed: 21570275]
43. Longtine MS, McKenzie A 3rd, Demarini DJ, Shah NG, Wach A, Brachat A, Philippsen P, Pringle JR. Additional modules for versatile and economical PCR-based gene deletion and modification in Saccharomyces cerevisiae. Yeast. 1998; 14(10):953–961. [PubMed: 9717241]
44. Katzmann DJ, Babst M, Emr SD. Ubiquitin-dependent sorting into the multivesicular body pathway requires the function of a conserved endosomal protein sorting complex, ESCRT-I. Cell. 2001; 106(2):145–155. [PubMed: 11511343]
45. Sherman, F.; Fink, GR.; Lawrence, LW. Methods in yeast genetics: a laboratory manual. Cold Spring Harbor, NY: Cold Spring Harbor Laboratory Press; 1979.
46. Babst M, Wendland B, Estepa EJ, Emr SD. The Vps4p AAA ATPase regulates membrane association of a Vps protein complex required for normal endosome function. Embo J. 1998; 17(11):2982–2993. [PubMed: 9606181]
47. Darsow T, Odorizzi G, Emr SD. Invertase fusion proteins for analysis of protein trafficking in yeast. Methods Enzymol. 2000; 327:95–106. [PubMed: 11044977]
48. Robinson JS, Klionsky DJ, Banta LM, Emr SD. Protein sorting in *Saccharomyces cerevisiae*: isolation of mutants defective in the delivery and processing of multiple vacuolar hydrolases. Mol Cell Biol. 1988; 8(11):4936–4948. [PubMed: 3062374]
49. Babst M, Sato TK, Banta LM, Emr SD. Endosomal transport function in yeast requires a novel AAA-type ATPase, Vps4p. EMBO J. 1997; 16(8):1820–1831. [PubMed: 9155008]
50. Horazdovsky BF, Busch GR, Emr SD. *VPS21* encodes a rab5-like GTP binding protein that is required for the sorting of yeast vacuolar proteins. EMBO J. 1994; 13(6):1297–1309. [PubMed: 8137814]
51. Strochlic TI, Schmiedekamp BC, Lee J, Katzmann DJ, Burd CG. Opposing activities of the Snx3-retromer complex and ESCRT proteins mediate regulated cargo sorting at a common endosome. Mol Biol Cell. 2008; 19(11):4694–4706. [PubMed: 18768754]

Synopsis

We constructed fusion proteins that bind to endosomes and interact with ESCRTs. The trafficking analysis of these proteins showed that binding to ESCRTs caused either recycling (mimicking ESCRT machinery) or mediated ubiquitin-independent sorting into the MVB pathway (mimicking cargo). Furthermore, efficient MVB sorting of soluble proteins was observed.

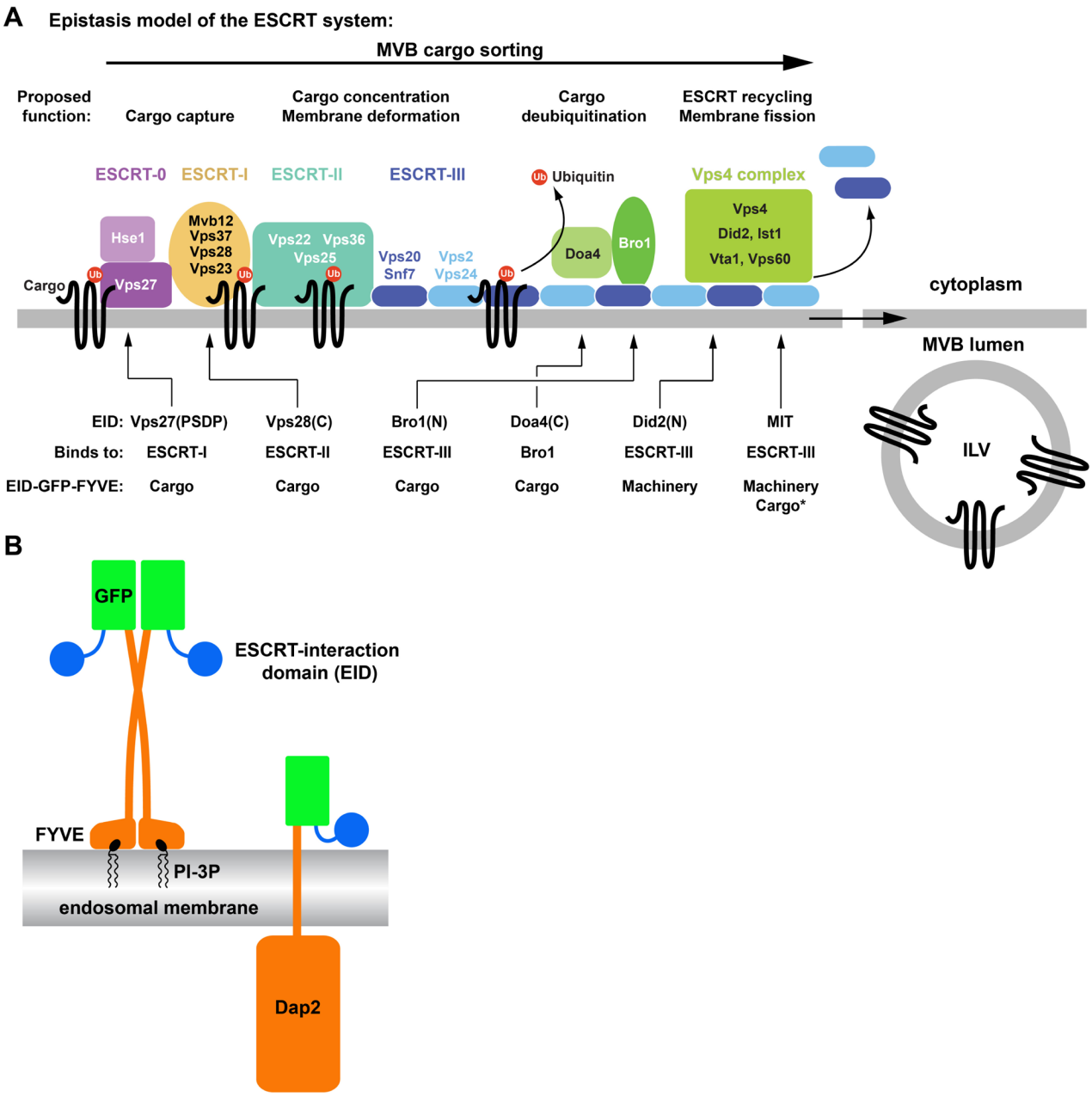

Figure 1.

The FYVE domain protein fusion constructs. (A) The currently proposed epistasis model for ESCRT function, from cargo capture to vesicle formation (ILV). The ESCRT-interaction domains (EIDs) used in this study and their effect on the localization of GFP-FYVE are indicated. (B) Schematic representation of the structures of the FYVE domain and Dap2 fusion constructs.

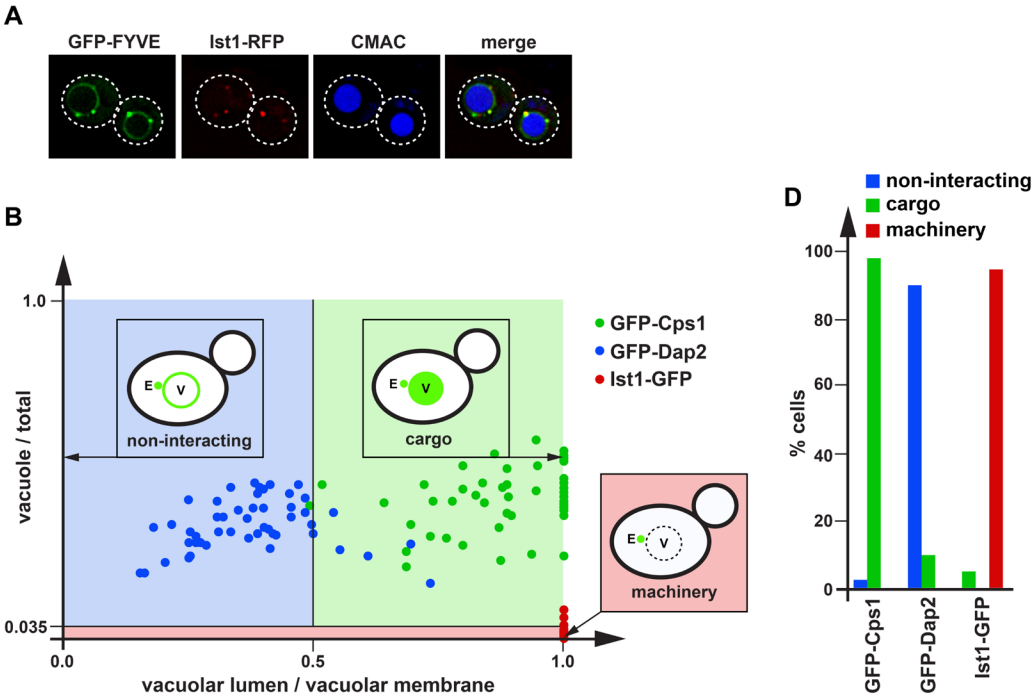

C

	intensities (arbitrary units)			ratios	
	endosome	vacuolar membrane	vacuolar lumen	vacuole / total	vacuolar lumen / vacuolar membrane
GFP-CPS	567	260*	260	0.48	1.00
GFP-Dap2	597	260	80	0.36	0.31
Ist1-GFP	3497	20*	20	0.01	1.00

Figure 2.

Quantitative analysis of the localization of GFP fusion constructs. (A) Fluorescence microcopy of GFP-FYVE and Ist1-RFP expressed in cells stained with the vacuolar marker CMAC. Dotted lines mark the outlines of the cells. (B) Cells expressing GFP-Cps1, GFP-Dap2 or Ist1-GFP were analyzed by microscopy and the resulting localization data was presented on a scatter plot (50 cells each). Based on the distribution of these standard proteins, three areas were defined representing non-interacting proteins, cargoes and ESCRT machinery-like proteins. (C) Example of the data analysis used to obtain the scatter plot shown in B. Asterisks indicate cases where the intensity of the vacuolar membrane was lower or equal to that of the vacuolar lumen and thus the value for the membrane was set to be identical to the value of the vacuolar lumen. (D) Bar graph representation of the data shown in B.

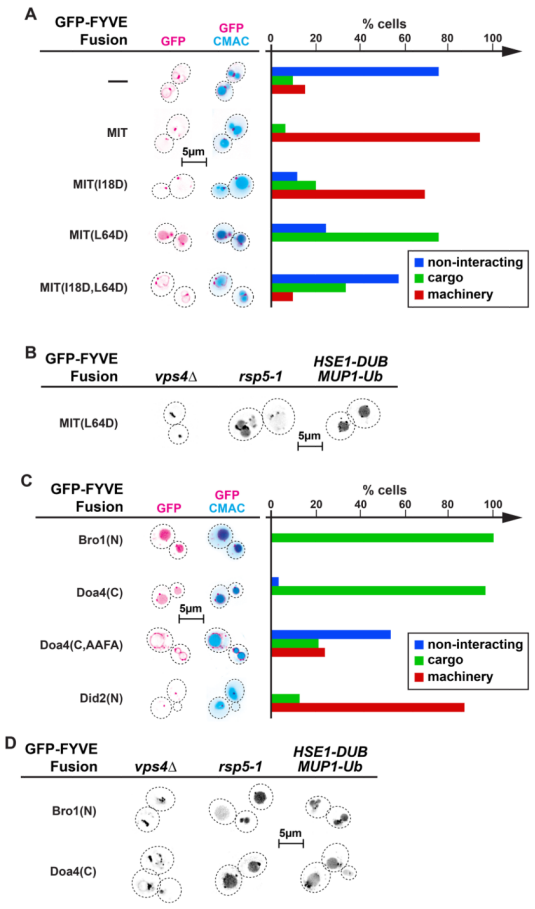

Figure 3.

Binding to ESCRT-III mediates either recycling or MVB sorting of GFP-FYVE fusion constructs. Fluorescence microscopy of cells expressing different ESCRT-III interacting GFP-FYVE fusion proteins. Dotted lines mark the outlines of the cells. The microscopy pictures were inverted. (A)(C) Cells were stained with the vacuolar marker CMAC. Quantification of the localization of the GFP-FYVE fusion constructs (50 cells each) based on the three behavior types defined in Figure 2B (non-interacting, cargo, machinery).

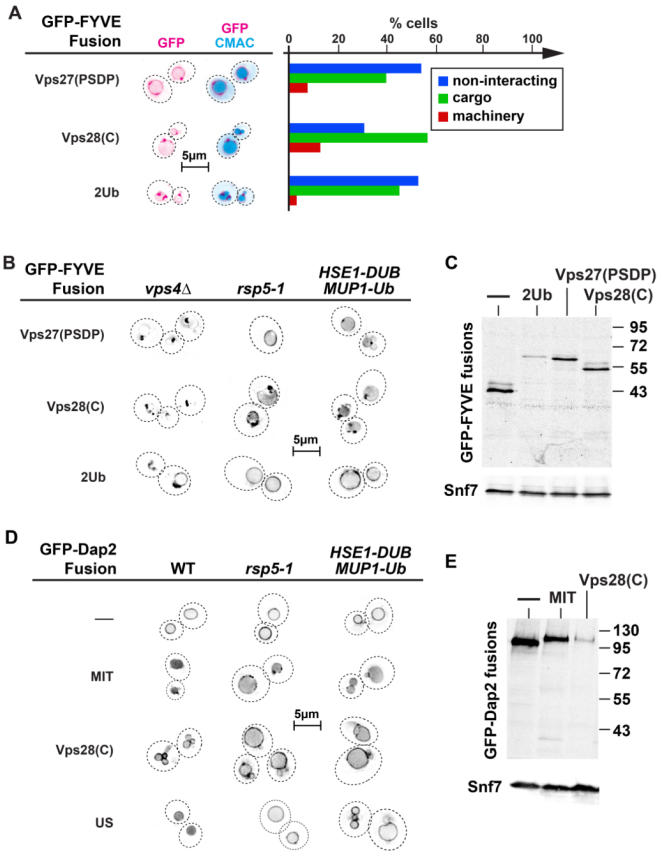

Figure 4.

Binding to ESCRTs can mediate ubiquitin-independent MVB sorting of both soluble and transmembrane cargo. (A)(B)(D) Fluorescence microscopy of yeast cells (outlined with dashed lines) expressing either GFP-FYVE or GFP-Dap2 fusion proteins. The fluorescence images were inverted. In A cells were stained with the vacuolar marker CMAC. Bar graph representing the localization behavior or GFP-FYVE fusion proteins interacting with the early ESCRT machinery (based on rules defined in Figure 2B, 50 cells each were analyzed). (C)(E) Western blot analysis of *vps4*Δ*pep4*Δ*prb1*Δ cells expressing different GFP-FYVE fusion constructs (anti-GFP). The ESCRT protein Snf7 served as a loading control.

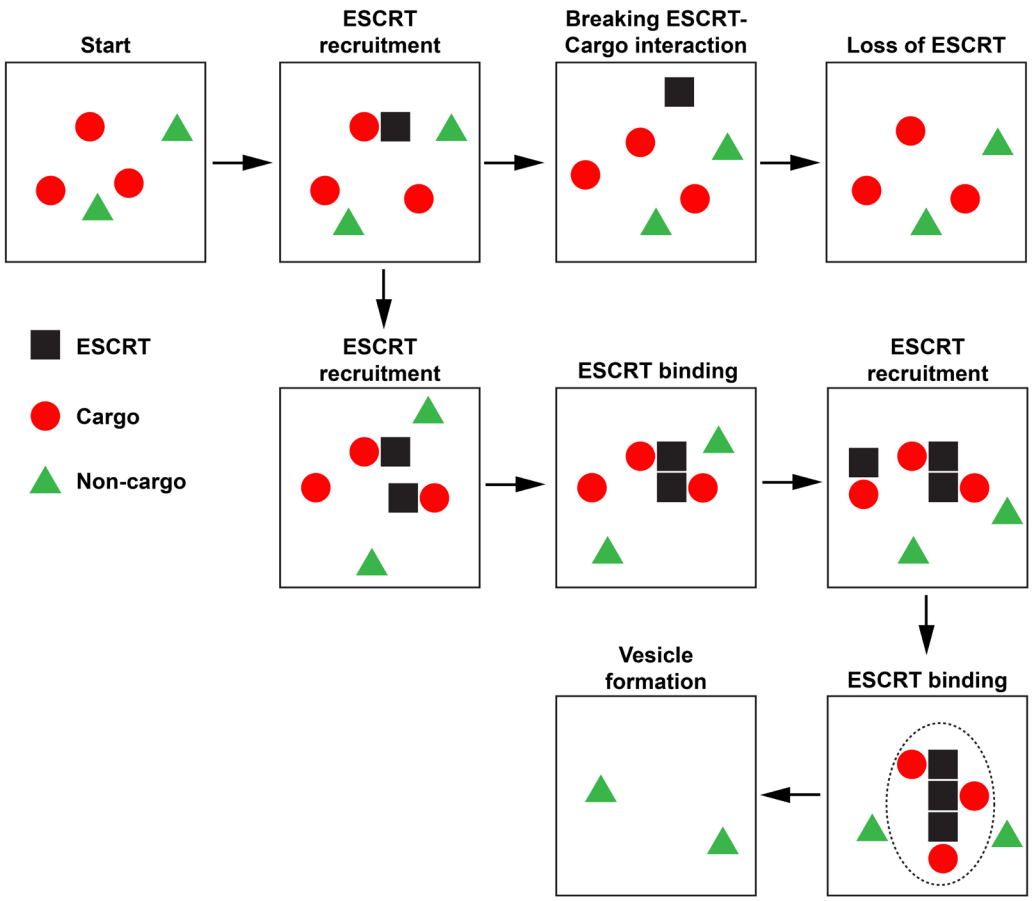

Figure 5.
Simplified example of the computer modeling used to test the proposed cargo-sorting model. The dotted line indicates the area that was removed during the vesicle formation step. For more information see the text.

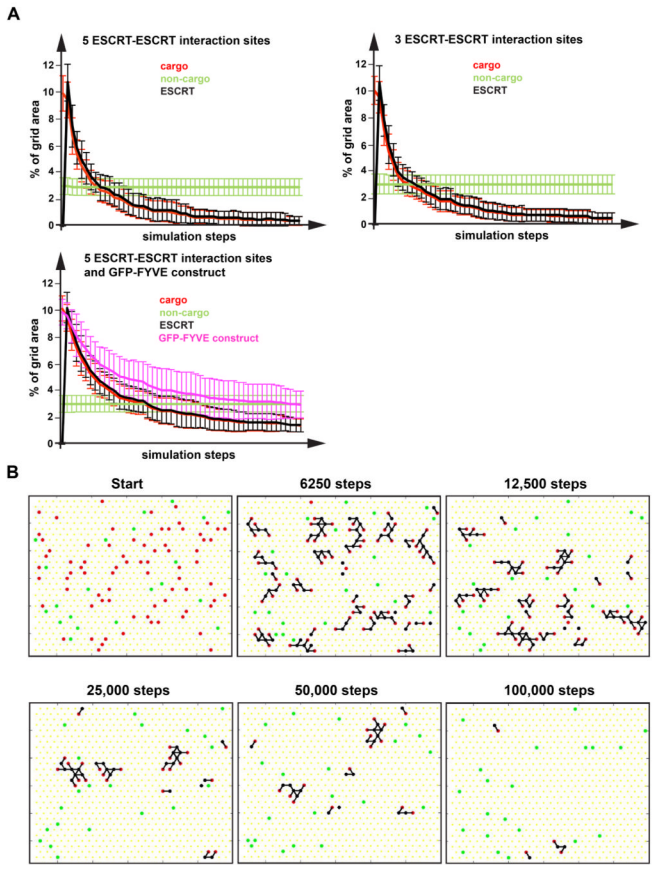

Figure 6.

In silico sorting of MVB cargo. A computer simulation of ESCRT-mediated cargo sorting was developed based on the rules listed in the text (for more detail see Materials and Methods). (A) The graphs show the sorting of cargo (indicated by the removal of cargo) averaged from 20 simulations as a function of simulation steps. The Y-axis indicates the % of the area occupied by the different components and thus represents concentration of that component on the membrane. (B) Snapshots of a simulation with five ESCRT-ESCRT interaction sites. Cargoes are in red, non-cargoes in green and ESCRT components in black. Black lines indicate interactions between components. A movie of this simulation can be found in Online Supplemental Material.

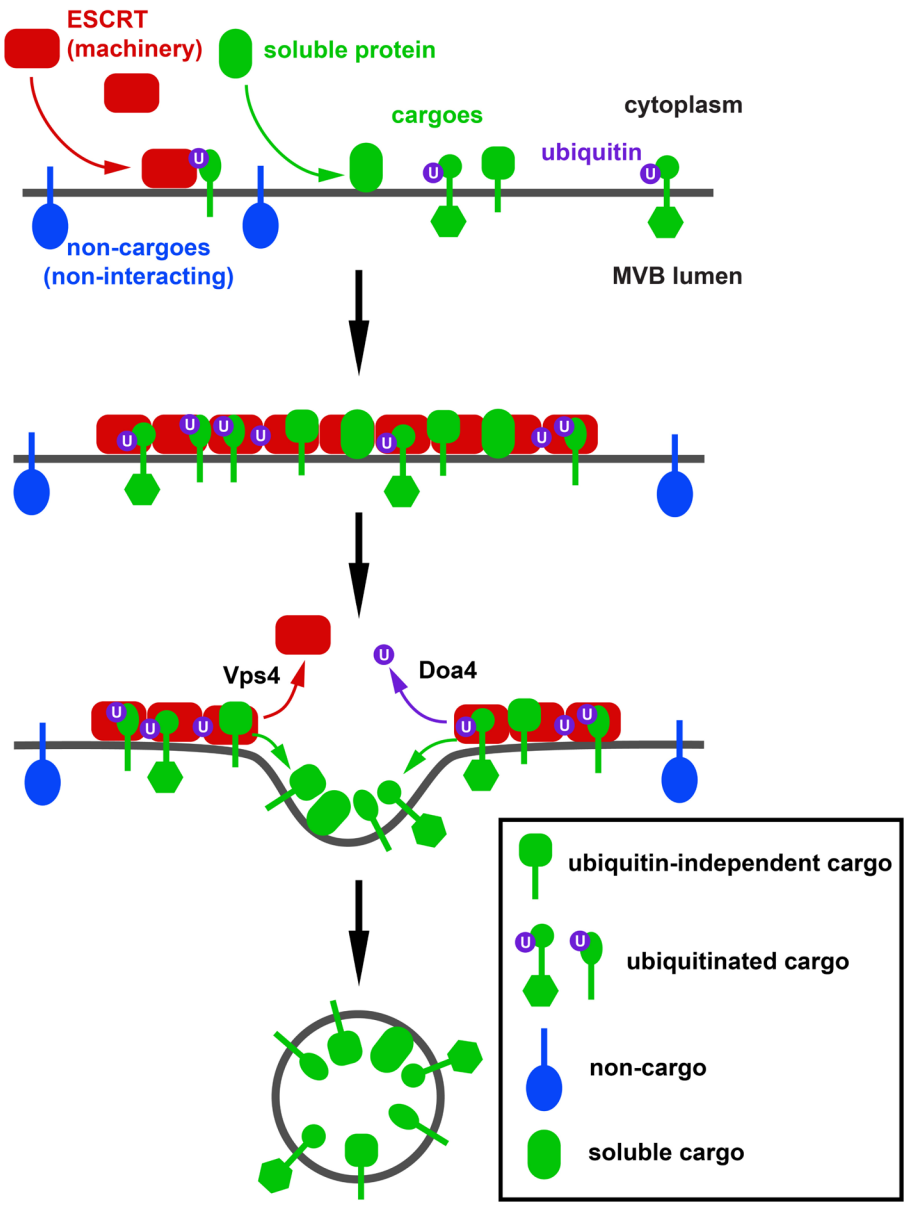

Figure 7.

Model for the ESCRT-mediated sorting of cargo into forming ILVs. ESCRTs and cargo proteins (transmembrane or soluble) assemble on the endosomal membrane into a protein network that is stabilized by ESCRT-ESCRT and ESCRT-ubiquitin interactions. Both cargo and ESCRTs can be tagged by ubiquitin. Transmembrane proteins that are not interacting with ESCRTs are sterically excluded from the network. Disassembly of the network by Vps4 and Doa4-dependent deubiquitination allows cargo to diffuse into the forming ILV whereas ESCRT components are released into the cytoplasm.

Table 1

Fusion proteins.

Name	Predicted Interaction	Observed Behavior (majority of cells)
GFP-FYVE	none	non-interacting
MIT-GFP-FYVE	ESCRT-III (MIM1, MIM2)	machinery
MIT(L64D)-GFP-FYVE	ESCRT-III (MIM2)	cargo
MIT(I18D)-GFP-FYVE	ESCRT-III (MIM1)	machinery
MIT(L64D,I18D)-GFP-FYVE	none	non-interacting
Bro1(N)-GFP-FYVE	ESCRT-III (Snf7)	cargo
GFP-Doa4(C)-FYVE	Bro1	cargo
GFP-Doa4(C,AAFA)-FYVE	none	non-interacting
Did2(N)-GFP-FYVE	ESCRT-III	machinery
Ub-GFP-FYVE-Ub	ESCRT-0, -I, -II	cargo/non-interacting
Vps27(PSDP)-GFP-FYVE	ESCRT-I	cargo/non-interacting
Vps28(C)-GFP-FYVE	ESCRT-II	cargo
GFP-Dap2	none	non-interacting
MIT-GFP-Dap2	ESCRT-III (MIM1, MIM2)	cargo
Vps28(C)-GFP-Dap2	ESCRT-II	cargo

Table 2

CPY-Invertase secretion assay.

Construct	% CPY-Invertase secretion (normalized values, average of three experiments)
Empty vector	0 ± 0.4
Vps4(E233Q)	100 ± 4.8
GFP-FYVE	6 ± 0.2
MIT-GFP-FYVE	6 ± 0.2
MIT(L64D)-GFP-FYVE	10 ± 0.3
MIT(I18D)-GFP-FYVE	10 ± 0.3
MIT(L64D,I18D)-GFP-FYVE	9 ± 0.3
Bro1(N)-GFP-FYVE	−6 ± 0.4
GFP-Doa4(C)-FYVE	−3 ± 0.6
GFP-Doa4(C,AAFA)-FYVE	−6 ± 0.4
Did2(N)-GFP-FYVE	−3 ± 0.5
2Ub-GFP-FYVE	18 ± 0.9
Vps27(PSDP)-GFP-FYVE	−2 ± 0.5
Vps28(C)-GFP-FYVE	−7 ± 0.2

Table 3

Strains and Plasmids used in this study

Strains or Plasmids	Descriptive name	Genotype or description	Reference or source
Strains			
SEY6210	WT	*MATα leu2-3,112 ura3-52 his3-Δ200 trp1-Δ901 lys2-801 suc2-Δ9 GAL*	(48)
MBY3	*vps4*Δ	SEY6210, *VPS4::TRP1*	(49)
MBY45	*doa4*Δ	SEY6210, *DOA4::HIS3*	This study
MBY52	*vps4*Δ *pep4*Δ *prb1*Δ	SEY6210, *PEP4,PRB1::LEU2, VPS4::TRP1*	(44)
BHY10	WT *CPY-I*	SEY6210, *leu2-3,112::pBHY11* (*CPY-Inv LEU2*)	(50)
JPY98	*rsp5*Δ *rsp5L733S*	SEY6210, *RSP5::HIS3*, pDsRedRSP5(L733S)	(51)
SKY10	*vps4*Δ *pep4*Δ *prb1*Δ	SEY6210, *PEP4,PRB1::LEU2, VPS4::G418*	This study
Plasmids			
pSD2	GFP-Cps1	*P(PRC1)*-GFP-*CPS1* (pRS415)	This study
pGO89	GFP-Dap2	*P(PRC1)*-GFP-*DAP2* (pRS426)	(44)
pSK11	GFP-Dap2	*P(PRC1)*-GFP-*DAP2* (pRS415)	This study
pMB331	Ist1-mCherry	*IST1*-mCherry (pRS416)	This study
pMB243	Ist1-GFP	*IST1*-GFP (pRS416)	(26)
pCB257	GFP-FYVE	*P(PRC1)*-GFP-linker2*-FYVE(EEA1) (pRS424)	(14)
pSK43	GFP-FYVE	*P(PRC1)*-GFP-linker2*-FYVE(EEA1) (pRS414)	This study
pSK27	MIT-GFP-FYVE	*vps4*(1-261)-linker3*-EGFP-linker2*- FYVE(EEA1) (pRS415)	This study
pSK34	MIT(L64D)-GFP-FYVE	*vps4*(1-261, *L64D*)-linker3*-EGFP-linker2*- FYVE(EEA1) (pRS415)	This study
pSK126	MIT(I18D)-GFP-FYVE	*vps4*(1-261, *I18D*)-linker3*-EGFP-linker2*- FYVE(EEA1) (pRS414)	This study
pSK82	MIT(I18D,L64D)-GFP- FYVE	*vps4*(1-261, *I18D, L64D*)-linker3*-EGFP-linker2*- FYVE(EEA1) (pRS414)	This study
pSK151	Bro1(N)-GFP-FYVE	*P(SNF7)*-linker12*-*bro1*(4-1161)-linker5*-EGFP- linker2*-FYVE(EEA1) (pRS416)	This study
pSW1	GFP-Doa4(C)-FYVE	*P(PRC1)*-GFP-linker4*-*doa4*(1684-end)-linker5*- FYVE(EEA1) (pRS416)	This study
pMC51	GFP-Doa4(C)-FYVE	*P(PRC1)*-GFP-linker4*-*doa4*(1684-end)-linker5*- FYVE(EEA1) (pRS424)	This study
pSK158	GFP-Doa4(C, AAFA)- FYVE	*P(PRC1)*-GFP-linker4*-*doa4*(1684-end, *Y826A, P827A, L829A*)-linker5*-FYVE(EEA1) (pRS416)	This study
pSK150	Did2(N)-GFP-FYVE	*P(SNF7)*-linker12*-*did2*(4-309)-linker6*-EGFP- linker2*-FYVE(EEA1) (pRS416)	This study
pSK141	Ub-GFP-FYVE-Ub	*P(SNF7)*-linker13*-*UB*(10-222)-linker7*-EGFP- linker2*-FYVE(EEA1)-linker8*-*UB*(10-222) (pRS416)	This study

Strains or Plasmids	Descriptive name	Genotype or description	Reference or source
pSK142	Ub-GFP-FYVE-Ub	*P(SNF7)*-linker13*-*UB*(10-222)-linker7*-EGFP- linker2*-FYVE(EEA1)-linker8*-*UB*(10-222) (pRS424)	This study
pSK95	Vps27(PSDP)-GFP-FYVE	*P(SNF7)*-linker13*-*vps27*(1303-1602)-linker1*- EGFP-linker2*-FYVE(EEA1) (pRS416)	This study
pSK96	Vps28(C)-GFP-FYVE	*P(SNF7)*-linker13*-*vps28*(442-726)-linker1*- EGFP-linker2*-FYVE(EEA1) (pRS416)	This study
pPL4012	HSE1-DUB	*P(CUP1)-HSE1*-UL36CD-3xHA (pRS316)	(16)
pSK153	Mup1-Ub	*P(CUP1)-MUP1*-linker11*-*UB*(4-222) (pRS425)	This study
pSK76	MIT-GFP-Dap2	*vps4*(1-261)-linker3*-EGFP-linker10*-*DAP2* (pRS414)	This study
pSK178	MIT-GFP-Dap2	*vps4*(1-261)-linker3*-EGFP-linker10*-*DAP2* (pRS426)	This study
pSK175	US-GFP-Dap2	*P(SNF7)*-linker13*-*CPS1*(13-33)-linker7*-EGFP- linker9*-*DAP2* (pRS426)	This study
pSK100	Vps28(C)-GFP-Dap2	*P(SNF7)*-linker13*-*vps28*(442-726)-linker1*- EGFP-linker9*-*DAP2* (pRS416)	This study
pMB66	Vps4(E233Q)	*vps4(E233Q)* (pRS413)	(46)

* linkers encode the following amino acid sequences: linker1 – GGGNS, linker2 – SGLRSRAHASNS, linker3 – LALPVAT, linker4 – SGPRS, linker5 – GNS, linker6 – NS, linker7 – AAANS, linker8 – AAG, linker9 – SR, linker10 – SGLRS, linker11 – GLA, linker12 – MRS, linker13 –MRSGG